Photon density of states for deformed surfaces

2006 J. Phys. A: Math. Gen. 39 6309

(http://iopscience.iop.org/0305-4470/39/21/S22)

INSTITUTE OF PHYSICS PUBLISHING JOURNAL OF PHYSICS A: MATHEMATICAL AND GENERAL

J. Phys. A: Math. Gen. **39** (2006) 6309–6316 doi:10.1088/0305-4470/39/21/S22

Photon density of states for deformed surfaces

T Emig

Institut für Theoretische Physik, Universität zu Köln, Zülpicher Straße 77, D-50937 Köln, Germany

E-mail: te@thp.uni-koeln.de

Received 23 November 2005, in final form 5 January 2006
Published 10 May 2006
Online at stacks.iop.org/JPhysA/39/6309

Abstract

A new approach to the Helmholtz spectrum for arbitrarily shaped boundaries and a rather general class of boundary conditions is introduced. We derive the boundary induced change of the density of states in terms of the free Green's function from which we obtain both perturbative and non-perturbative results for the Casimir interaction between deformed surfaces. As an example, we compute the lateral electrodynamic Casimir force between two corrugated surfaces over a wide parameter range. Universal behaviour, fixed only by the largest wavelength component of the surface shape, is identified at large surface separations. This complements known short distance expansions which are also reproduced.

PACS numbers: 42.25.Fx, 03.70.+k, 12.20.−m, 42.50.Ct

(Some figures in this article are in colour only in the electronic version)

1. Introduction

Casimir interactions can be viewed as a consequence of a change in the photon spectrum under a relative displacement of the interacting objects. For two parallel ideal metallic plates, the change in the photon density of states (DOS) with the plate distance H is well known [1]. It is peaked close to the characteristic frequency $\omega \sim c/H$ which provides the dominant contribution to the interaction. However, even for simple geometries like a plate and a sphere no exact expression for the change in the DOS is available. The reason for this is the difficulty in computing the distribution of eigenfrequencies of the Helmholtz wave equation in arbitrary geometries. This is inherently linked to the problem of chaotic (quantum) billiards [2]. For Casimir interactions, the natural question arises: To what extent the force characterizes the shape of the interacting objects and vice versa? There is a long debate about the existence of a repulsive Casimir interaction between ideal metals, which was mainly initiated by the positivity of the Casimir energy of a single infinitesimal thin sphere of ideal metal [3]. So far, no example of a repulsive force between two separated ideal metallic bodies has been found.

During the past few decades, a number of approximative methods have been developed to determine the Casimir interaction in more complicated geometries. These include the proximity and pairwise additivity approximations [4], semiclassical approaches [5], multiple scattering expansions [1] and, more recently, a simple to implement optical approach [6] which is expected to work at sufficiently small separations but has been applied also at larger distances to study thermal corrections [7]. Despite the usefulness of these approaches in certain limits, reliable results for the entire range of energies (or distances) are not known in general. Here I shall present a formula for the density of states in terms of the free space Green's function which is evaluated at the (ideal metallic) surfaces only. This formula will be used to compute the DOS for two deformed surfaces both perturbatively in the deformations and also exactly with the aid of a previously developed numerical method for periodic surfaces [8]. As an application, we study the lateral force between periodic surfaces. It is found that the surface's shape can be deduced from the force at short distances whereas at large separations universality prevails.

2. Trace formula for the photon spectrum

For geometries with a translational invariant direction the electromagnetic field splits into transverse electric (TE) and magnetic (TM) modes. Both modes are described by a scalar field which fulfils either Dirichlet or Neumann boundary conditions on the ideal metal surfaces. Hence, we consider in the following the scalar field Helmholtz equation

$$(\nabla^2 + k^2)\phi(\mathbf{x}) = 0. \tag{1}$$

The relevant quantity for the Casimir interaction is the *change* $\delta\rho(k) = \rho(k) - \rho_\infty(k)$ in the DOS caused by moving the surfaces from infinity to the finite distance for which one is interested in the Casimir energy. Hence $\rho_\infty(k)$ is the DOS for infinitely separated surfaces. The relevant finite part of the zero-point energy is then given by the sum of $k\delta\rho(k)$ over k. It is more convenient to work in Euclidean space by performing a Wick rotation to imaginary frequencies. With $\delta\tilde{\rho}(q_0) = -\delta\rho(iq_0)$ the Casimir energy becomes

$$\mathcal{E} = \frac{\hbar c}{2}\int_0^\infty \mathrm{d}q_0\, q_0\, \delta\tilde{\rho}(q_0). \tag{2}$$

In order to derive the DOS we start with the four-dimensional Euclidean action

$$S = \frac{1}{2}\int \mathrm{d}^4X\,(\nabla\phi)^2. \tag{3}$$

Using a path-integral formulation with delta-functions enforcing the boundary conditions on the surfaces S_α [9], one obtains the two-point correlation function in the presence of boundaries [10]. With the free space Green's function $G_0(\mathbf{x}, \mathbf{x}'; q_0) = \mathrm{e}^{-q_0|\mathbf{x}-\mathbf{x}'|}/(4\pi|\mathbf{x}-\mathbf{x}'|)$, the modified correlation $G(\mathbf{x}, \mathbf{x}'; q_0) = \langle\phi_{q_0}(\mathbf{x})\phi_{-q_0}(\mathbf{x}')\rangle$ in the presence of boundaries is given by

$$\begin{aligned} G(\mathbf{x}, \mathbf{x}';q_0) - G_0(\mathbf{x}, \mathbf{x}';q_0) = -\sum_{\alpha\beta}\int \mathrm{d}\mathbf{u}\,\mathrm{d}\mathbf{u}'\, G_0(\mathbf{x}, \mathbf{s}_\alpha(\mathbf{u});q_0) \\ \times \mathcal{M}^{-1}_{\alpha\beta}(\mathbf{u}, \mathbf{u}';q_0) G_0(\mathbf{x}', \mathbf{s}_\beta(\mathbf{u}');q_0), \end{aligned} \tag{4}$$

where $\mathcal{M}^{-1}_{\alpha\beta}(\mathbf{u}, \mathbf{u}';q_0)$ is the functional inverse of $\mathcal{M}_{\alpha\beta}(\mathbf{u}, \mathbf{u}'; q_0) = G_0(\mathbf{s}_\alpha(\mathbf{u}), \mathbf{s}_\beta(\mathbf{u}'); q_0)$ with the three-dimensional (3D) vectors $\mathbf{s}_\alpha(\mathbf{u})$ denoting the positions of surface S_α as a function of the two-dimensional (2D) coordinate $\mathbf{u}$. This result applies to Dirichlet boundary conditions. For the Neumann case, G_0 has to be replaced by $\partial_{\mathbf{n}_\alpha(\mathbf{u})}G_0(\mathbf{x}, \mathbf{s}_\alpha(\mathbf{u});q_0)$ on the right-hand side of equation (4) and $\mathcal{M}_{\alpha\beta}(\mathbf{u}, \mathbf{u}'; q_0) = \partial_{\mathbf{n}_\alpha(\mathbf{u})}\partial_{\mathbf{n}_\beta(\mathbf{u}')}G_0(\mathbf{s}_\alpha(\mathbf{u}), \mathbf{s}_\beta(\mathbf{u}'); q_0)$ with $\partial_{\mathbf{n}_\alpha}$ the normal

derivative at the surface S_α. Next, we make use of the property that the trace of Green's function yields the DOS. In the Euclidean formulation this relation reads

$$\rho(\mathrm{i}q_0) = \frac{2q_0}{\pi}\int \mathrm{d}^3\mathbf{x}\, G(\mathbf{x},\mathbf{x};q_0). \tag{5}$$

Here the spatial integration extends over all inner and outer regions of the surfaces. Since equation (4) holds in any spatial region, we obtain the change in the DOS by integrating the right-hand side of this equation with $\mathbf{x} = \mathbf{x}'$ running over the entire 3D space. The integration is easy to perform in momentum space since $\mathbf{x}$ and $\mathbf{x}'$ occur as arguments of the free Green's function in equation (4). Using for the Fourier transformed propagator $\partial/\partial q_0\big(q_0^2+q^2\big)^{-1} = -2q_0\big(q_0^2+q^2\big)^{-2}$, one obtains after $\mathbf{x}$-integration, both for $\mathcal{M}$ and $\mathcal{M}_\infty$, the final trace formula

$$\delta\tilde{\rho}(q_0) = -\frac{1}{\pi}\frac{\partial}{\partial q_0}\mathrm{Tr}\ln\left(\mathcal{M}\mathcal{M}_\infty^{-1}\right). \tag{6}$$

The trace runs over the 2D coordinates $\mathbf{u}$ and the surface indices α. An advantage of this formula is its independence of surface self-energies which diverge in the limit of ideal metals but are irrelevant for the interaction. It is important to note that this formula can be applied in any spatial dimension and also to other types of boundary conditions which can be implemented via delta-functions in the path integral [11].

3. Density of states

In this section, we will apply the trace formula of equation (6) to two deformed but on average parallel plates. In the first part, we study (in amplitude and curvature) small deformations of general shape (corresponding to the large distance limit) by perturbation theory. Non-perturbative numerical results for the DOS of periodically corrugated surfaces with edges at closer distances are presented in the second part.

3.1. Perturbation theory for arbitrarily deformed surfaces

Let us consider two parallel surfaces with small deformations which are parametrized by $\mathbf{s}_1(\mathbf{u}) = (\mathbf{u}, h_1(\mathbf{u}))$ and $\mathbf{s}_2(\mathbf{u}) = (\mathbf{u}, H + h_2(\mathbf{u}))$ where the deformation fields h_α are small compared to the mean distance H. We are interested in the deformation induced modification of the flat surface DOS

$$\delta\tilde{\rho}_0(q_0) = \frac{q_0}{2}\log(1-\mathrm{e}^{-2q_0H})A, \tag{7}$$

where A is the surface area. Expanding the kernel $\mathcal{M} = \mathcal{M}_0 + \delta\mathcal{M}$ with $\mathcal{M}_0$ the kernel for flat surfaces and $\delta\mathcal{M}$ the correction due to the deformations, one finds for the change of the DOS

$$\delta\tilde{\rho}(q_0) = -\frac{1}{\pi}\mathrm{Tr}\left[\log\mathcal{M}_0 + \log\left(1+\mathcal{M}_0^{-1}\delta\mathcal{M}\right)\right] - (H\to\infty), \tag{8}$$

where the contribution for $H\to\infty$ has to be subtracted. Expanding the logarithm to second order in the deformations $h_\alpha(\mathbf{u})$, the change of the DOS can be written as

$$\begin{aligned}\delta\tilde{\rho}(q_0) = \delta\tilde{\rho}_0(q_0) &- \frac{1}{4\pi^2}\frac{q_0^3}{\sinh^2(q_0H)}\int_{\mathbf{u}}\left[h_1^2(\mathbf{u})+h_2^2(\mathbf{u})\right]\\ &+ \int_{\mathbf{u},\mathbf{u}'}\left\{\frac{1}{2}\sum_\alpha K_\parallel(q_0;\mathbf{u}-\mathbf{u}')[h_\alpha(\mathbf{u})-h_\alpha(\mathbf{u}')]^2\right.\\ &\left.+\sum_{\alpha\neq\beta}K_\times(q_0;\mathbf{u}-\mathbf{u}')h_\alpha(\mathbf{u})h_\beta(\mathbf{u}')\right\},\end{aligned} \tag{9}$$

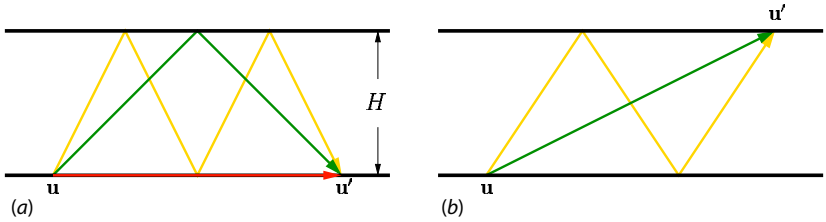

Figure 1. Graphical representation of the contributions to the kernels $K_\parallel$ (*a*) and $K_\times$ (*b*); cf equation (11).

where $\delta\tilde{\rho}_0$ is given by equation (7). The kernels of the non-local contributions can be expressed in terms of the free Green's function. In the following, we will focus due to limitations in space on Dirichlet conditions; the Neumann case has the form of equation (9), however with different kernels. Defining the series

$$R_{\rm even}(q_0;u)=\sum_{n=1}^{\infty}\frac{G_0(\sqrt{u^2+(2nH)^2};q_0)}{(2n)^2},$$
$$R_{\rm odd}(q_0;u)=\sum_{n=1}^{\infty}\frac{G_0(\sqrt{u^2+((2n-1)H)^2};q_0)}{(2n-1)^2} \tag{10}$$

the kernels can be written as

$$K_\parallel(q_0;\mathbf{u})=-\frac{8}{\pi}\partial_{q_0}\left[\left(\frac{1}{u}\partial_u G_0(u;q_0)+\partial_H^2 R_{\rm even}(q_0;u)\right)\partial_H^2 R_{\rm even}(q_0;u)\right]$$
$$K_\times(q_0;\mathbf{u})=-\frac{8}{\pi}\partial_{q_0}\left[\partial_H^2 R_{\rm odd}(q_0;u)\right]^2. \tag{11}$$

The contributions to the kernels can be viewed as multiple scattering paths between flat surface positions. The kernel $K_\parallel$ has only contributions from an even number of paths crossing the gap, connecting two positions on the same surface; see figure 1(*a*). The first factor $\sim\partial_u G_0$ in $K_\parallel$ is represented as a non-crossing paths. An odd number of crossing paths yield the kernel $K_\times$; see figure 1(*b*). Each path is associated with the free Green's function which is reduced by a factor which is the inverse squared number of gap crossings; cf equation (10).

3.2. Non-perturbative treatment of periodic surfaces

The above perturbative treatment is limited to small and smooth deformations. However, the trace formula turns out to be useful also in the case of surfaces with edges, and at large deformation amplitudes. Recently, a numerical tool has been developed to evaluate the Casimir force for periodic surface deformations [8]. Here we shall demonstrate that the same approach can also be applied to the DOS. Specifically, we consider uniaxial rectangular surface profiles shown in figure 3(*a*). In this section we restrict the analysis to no lateral shift, $b=0$. By Fourier transforming $\mathcal{M}_{\alpha\beta}(\mathbf{u},\mathbf{u}';q_0)$ with respect to $\mathbf{u}$ and $\mathbf{u}'$ one can employ the periodicity of the surface profiles (along the x_1-direction) which leads to the representation

$$\tilde{\mathcal{M}}_{\alpha\beta}(\mathbf{p},\mathbf{q};q_0)=(2\pi)^2\delta(p_2+q_2)\sum_{m=-\infty}^{\infty}\delta(p_1+q_1+2\pi m/\lambda)N_m^{\alpha\beta}(q_1,q_2;q_0), \tag{12}$$

which defines the 2×2 matrices N_m that can be computed analytically and are given in [8] for the present geometry. $\tilde{\mathcal{M}}$ can be transformed to block-diagonal form so that each block couples only waves whose momenta differ from a given Bloch momentum by integer multiples of $2\pi/\lambda$. This decomposition can be used to define the function

$$g(q_1, q_2; q_0) = \mathrm{Tr}\left(B^{-1}\partial_{q_0}B - B_\infty^{-1}\partial_{q_0}B_\infty\right) \tag{13}$$

where the trace runs over all discrete indices of the matrix $B_{kl}^{\alpha\beta}(q_1, q_2; q_0) = N_{k-l}^{\alpha\beta}(q_1 + 2\pi l/\lambda, q_2; q_0)$, and B_∞ is the analogue of $\mathcal{M}_\infty$, i.e., B for $H \to \infty$. For practical computations, we take $k, l = -M, \ldots, M$ with an integer cutoff M which should be taken to infinity. The change of the DOS can then be expressed as

$$\delta\tilde{\rho}(q_0) = -\frac{A}{4\pi^3}\int_{-\infty}^{\infty} \mathrm{d}q_2 \int_0^{2\pi/\lambda} \mathrm{d}q_1 g(q_1, q_2; q_0). \tag{14}$$

The following results for *electromagnetic* fluctuations are based on the application of this formula to Dirichlet (TM modes) and Neumann (TE modes) boundary conditions where the inversion of B, the trace in equation (13) and the integration are performed numerically.

Figure 2 displays the change of the DOS separately for TM and TE modes at the fixed distance $H = 10a$ and λ ranging from a to $100a$. The analytic expression for *flat* plates at the same mean distance and at the reduced distance $H - 2a$ is also plotted. An expected feature of these results is that the dominant contribution to the change of the DOS comes from frequencies $q_0 \sim H^{-1}$. For small modulation lengths $\lambda \ll H$ one can expect that for $q_0 \lesssim \lambda^{-1}$ the modes cannot probe the narrow valleys of the surface, and the DOS should be well described by the result for flat plates at a reduced distance $H - 2a$. While this is fully confirmed for TE modes, the magnetic modes show an unexplained deviation at sufficiently small q_0; see figure 3(*a*). For $\lambda \sim H$, figure 3(*b*), no significant differences between the two types of modes are observed, and the change of the DOS is in between the result for flat surfaces at distances H and $H - 2a$, respectively. For large $\lambda \gg H$, figure 3(*c*), there is a low density of edges, and one can expect the DOS for flat plates at distance H to be a good approximation. Such behaviour is indeed observed with a small decrease for TM and a small increase for TE modes close to the peak.

4. Universality of the lateral Casimir force

Finally, we use the previous results to study the Casimir force for the geometry in figure 3(*a*) which emerges from the variation of the zero-point energy with the shift b. The energy can be obtained from the DOS via equation (2). Without giving further details we note that the lateral force $F_l = -\partial\mathcal{E}/\partial b$ can be obtained by computing directly the derivative of the matrices $N_m^{\alpha\beta}$ in equation (12) with respect to b. The results are shown as a function of the surface distance for a fixed $b = \lambda/4$ in figure 3(*c*) and at a fixed $H = 10a$ as a function of b in figure 3(*d*). Let us compare our numerical results to approximative methods for small H. The proximity force approximation [4] yields the lateral force $F_{\mathrm{PFA}} = A[2\mathcal{E}_0(H) - \mathcal{E}_0(H - 2a) - \mathcal{E}_0(H + 2a)]/\lambda$ for $0 < b < \lambda/2$ with $\mathcal{E}_0(H) = -(\pi^2/720)\hbar c/H^3$, which changes sign at $b = \lambda/2$ discontinuously. The pairwise summation (PWS) of Casimir–Polder potentials $U(r) = -(\pi/24)\hbar c/r^7$ is often naively applied to metals, using a 'corrected' amplitude so as to reproduce the correct result for flat ideal metal plates [4]. For the present geometry F_{PWS} can be computed by a simple numerical integration. The two approximations are also shown in figures 3(*c*) and (*d*). For small δ, both approximations agree and match our

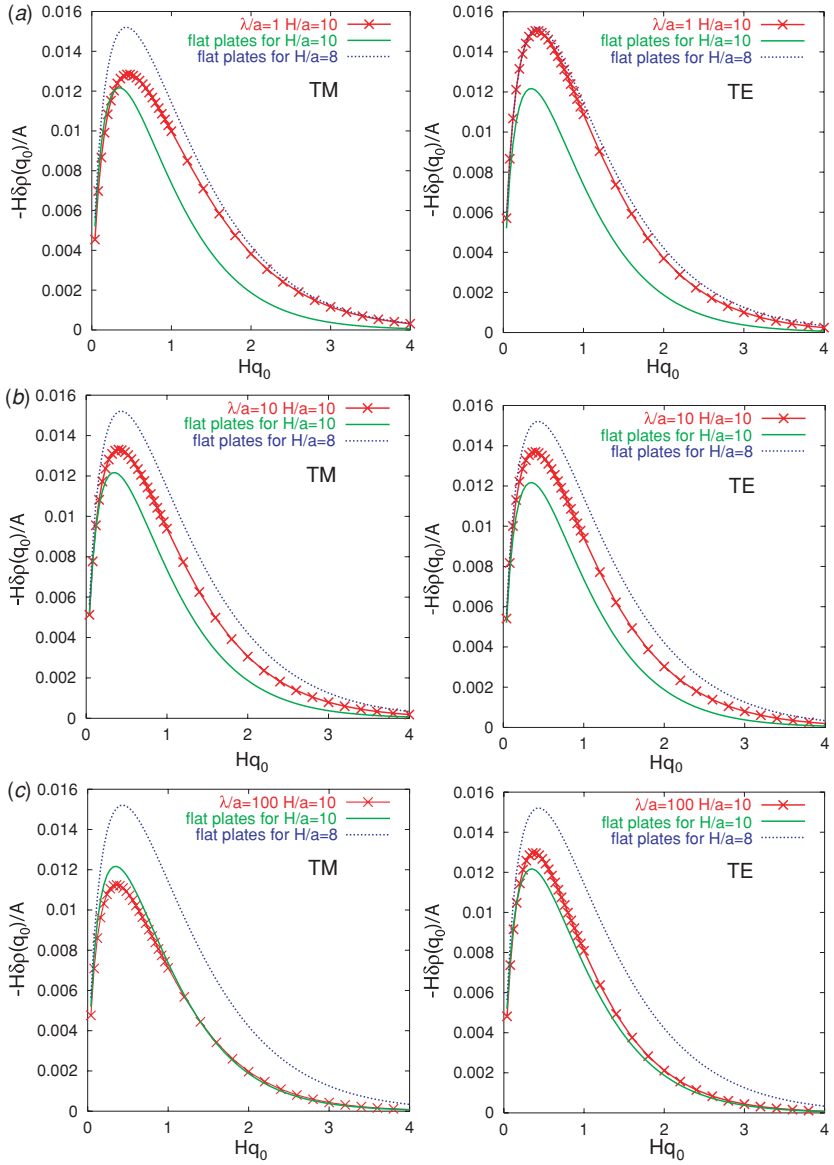

Figure 2. Change of the density of states $\delta\rho(q_0)$ per unit area for TM and TE modes with parameters $H = 10a$ and $\lambda/a = 1$ (a), 10 (b), 100 (c). The results were obtained with a cutoff of $M = 13$. (For scaling of the (Hq_0)-axis, $H = 10a$.)

results. Beyond $\delta \gtrsim \lambda/20$ the PFA starts to fail since it does not capture the exponential decay of $F_{\rm lat}$ for increasing δ. The PWS approach has a slightly larger validity range (cf figure 3(b)) and reproduces the exponential decay. However, it deviates by at least *one order of magnitude* from $F_{\rm lat}$ for $\delta \gtrsim 2.5\lambda$.

At large $\delta \gtrsim \lambda$ the lateral force shows universal behaviour in the form of approaching a limiting form which is independent of the detailed shape of the surface corrugation. The

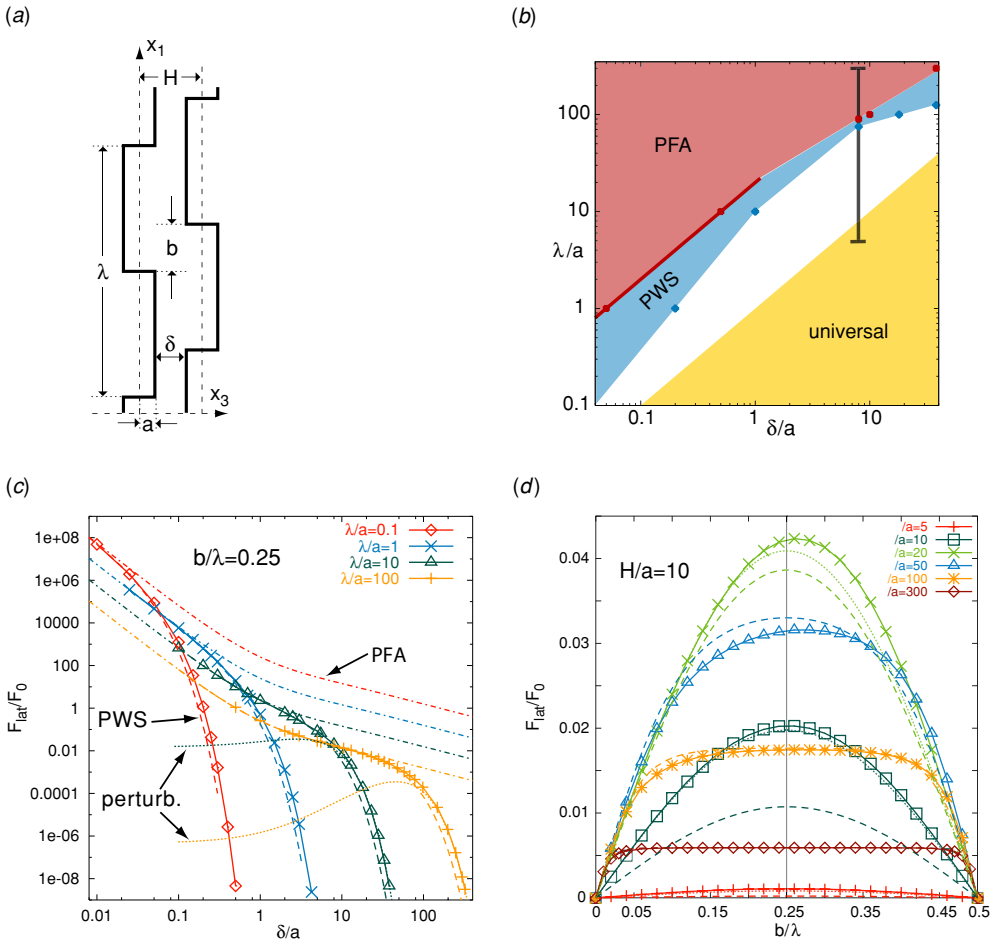

Figure 3. (*a*) Two plate geometry. (*b*) Approximate validity ranges of PFA and PWS, and the universal parameter range. The vertical bar marks the parameter range for λ/a in (*d*). (*c*) Lateral force (in units of the normal force $F_0(d)$ between flat surfaces). The PFA (dash-dotted), PWS (dashed) and the universal limit $F_{\rm pt}$ (dotted) are also shown. (*d*) Shape dependence of the lateral force. The dashed and the dotted curves are the PWS and the full perturbative result of [12], respectively.

universal limit is given by the lateral force for a *sinusoidally* shaped surface (with amplitude a_0 and wavelength λ) [12],

$$F_{\rm pt} = \frac{8\pi^3\hbar c}{15}\frac{a_0^2 A}{\lambda^5 H}\sin\left(\frac{2\pi}{\lambda}b\right)\mathrm{e}^{-2\pi H/\lambda}, \tag{15}$$

which is expected to hold for $a_0 \ll \lambda$. Using the lowest harmonic of the present rectangular geometry, corresponding to $a_0 = 4a/\pi$, we find indeed excellent agreement between $F_{\rm pt}$ and our results for the geometry of figure 3(*a*) for large $\delta \gtrsim \lambda$; see figure 3(*c*).

For the dependence on b, see figure 3(*d*), three regimes can be identified. For $\lambda \gg H$, the force profile resembles almost the rectangular shape of the surfaces, and the PWS approach yields consistent results. For decreasing λ, yet larger than H, the force profile becomes asymmetric with respect to $b = \lambda/4$ and more peaked, signaling the crossover to the universal

regime for $\lambda \lesssim H$ where the force profile becomes sinusoidal. We note that the PWS approach fails to predict the asymmetry of the force profile, and the PFA even predicts no variation for $0 < b < \lambda/2$. Finally, it should be noted that the range of validity for the universal form of equation (15) is not fully realized in the first experiment on lateral Casimir forces [13] where $H/a \approx 10$ and $\lambda/a \approx 55$ when a is set to the geometric mean of the different amplitudes for the two surfaces. It would be very useful to probe the predicted universality in experiments with different surface shapes and at larger H/λ.

Acknowledgment

Support through the Emmy–Noether Program of the DFG under grant no EM70/2 is acknowledged.

References

[1] Balian R and Duplantier B 1978 *Ann. Phys., NY* **112** 165
[2] Cvitanović P *et al* 2003 *Chaos: Classical and Quantum* (Copenhagen: Niels Bohr Institute) (chaosBook.org)
[3] Boyer T 1974 *Phys. Rev.* A **9** 2078
[4] Bordag M, Mohideen U and Mostepanenko V M 2001 *Phys. Rep.* **353** 1
[5] Schaden M and Spruch L 1998 *Phys. Rev.* A **58** 935
[6] Jaffe R L and Scardicchio A 2004 *Phys. Rev. Lett.* **92** 070402
[7] Scardicchio A and Jaffe R L 2005 *Preprint* quant-ph/0507042
[8] Büscher R and Emig T 2004 *Phys. Rev.* A **69** 062101
[9] Li H and Kardar M 1992 *Phys. Rev.* A **46** 6490
[10] Büscher R and Emig T 2005 *Phys. Rev. Lett.* **94** 133901
[11] Büscher R and Emig T 2004 *Nucl. Phys.* B **696** 468
[12] Emig T, Hanke A, Golestanian R and Kardar M 2003 *Phys. Rev.* A **67** 022114
[13] Chen F, Mohideen U, Klimchitskaya G L and Mostepanenko V M 2002 *Phys. Rev. Lett.* **88** 101801